

# Iterative Soft Decoding of Reed-Solomon Tail-Biting Convolutional Concatenated Codes

Jianchao Ye †, Ting-Yi Wu ‡, Jiongyue Xing †, Li Chen †

† School of Electronics and Information Technology, Sun Yat-sen University, Guangzhou, China

‡ School of Electronics and Communication Engineering, Sun Yat-sen University, Guangzhou, China

Email: yejch9@mail2.sysu.edu.cn, mavericktywu@gmail.com, xingjyue@mail2.sysu.edu.cn, chenli55@mail.sysu.edu.cn

**Abstract**—Reed-Solomon tail-biting convolutional concatenated (RS-TBCC) codes are investigated in this paper, aiming to eliminate the rate loss caused by the tail bits of the traditional RS convolutional concatenated (RS-CC) codes. The iterative soft decoding (ISD) for the RS-TBCC code is proposed, which integrates the tail-biting maximum *a posteriori* (TB-MAP) decoding algorithm for the inner tail-biting convolutional (TBC) code and the adaptive belief propagation (ABP) decoding algorithm for the outer RS codes. The proposed decoding is able to obtain significant performance gains through iterations. The outer decoding output will be validated by the maximum likelihood (ML) criterion, which alters the feedback to the inner decoding. However, the effectiveness of ML assessment degrades as the outer codeword length decreases. Therefore, a modified ISD is also proposed for shorter RS-TBCC codes in which smaller RS codes are employed.

**Index Terms**—concatenated codes, Reed-Solomon codes, tail-biting convolutional codes, iterative decoding

## I. INTRODUCTION

Future communication networks will be embedded by the features of ultra reliability and ultra low latency [1] [2]. Codes of short-to-moderate length, which have the potential of yielding a low latency and high performance, become the promising candidates for future networks [3].

Reed-Solomon convolutional concatenated (RS-CC) codes have been demonstrated to have low complexity and high reliability features [4], in which multiple RS codes serve as the outer codes and a convolutional code serves as the inner code. Between the outer and inner codes, the RS coded symbols are interleaved. The advantages of such a concatenated coding system include: 1) It can cope with a large variety of error patterns, since the inner code is good at correcting random errors [4] while the outer codes are good at correcting burst errors; 2) Efficient decoding algorithms exist for both the inner and outer codes.

However, in short-to-moderate blocklength regime, RS-CC codes would suffer a significant rate loss due to the necessity of the tail bits for the inner code. By initializing shift registers of the convolutional code with the last information bits, so called tail-biting, the tail bits can be removed to avoid rate loss without sacrificing the performance [5]. However, the tail-biting structure requires finding the initial state of the shift registers, which could result in a dramatic rise in complexity. Hence, RS-TBCC codes performance advantage (due to its higher rate) will be at the cost of decoding complexity.

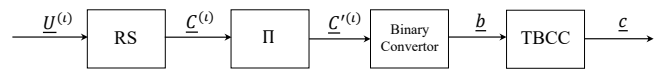


Fig. 1. Block diagram of the RS-TBCC encoder.

The RS-TBCC code was proposed in [6], in which the Viterbi decoder for tail-biting convolutional (TBC) code and the collaborative decoder for the interleaved RS code were employed to form a non-iterative decoder. To fully exploit the advantages of concatenated codes, iterative decoding should be employed to effectively exchange soft information between the inner and outer decoders. The iterative soft decoder for RS-CC codes was proposed in [7], which yields a significant coding gain over the conventional non-iterative Viterbi-Berlekamp-Massey (Viterbi-BM) decoder. For TBC codes, by extending a few sections of the tail-biting supertrellis, the wrap-around Viterbi algorithm (WAVA) can achieve a near-optimal performance with a low complexity [8]. A wrap-around maximum *a posteriori* (MAP) decoding algorithm was then devised in [9] to realize the SISO decoding of TBC codes, namely the TB-MAP decoding. For RS codes, the adapted belief propagation (ABP) decoder is a relatively efficient SISO decoder which yields a competent decoding performances [10].

This paper investigates the RS-TBCC code and proposes its iterative decoding algorithm. The proposed RS-TBCC decoder adopts the TB-MAP decoding [9] for the inner TBC code and the ABP decoding [10] for the outer RS codes, constituting an iterative decoding mechanism. In particular, the outer RS codes are decoded by the ABP-BM algorithm. If the BM decoding succeeds, it will feed back deterministic information for the inner TB-MAP algorithm, otherwise the extrinsic information will be fed back. Therefore, the outer decoding output validation is important, for which we employ the maximum likelihood (ML) criterion of [11]. However, the accuracy of this validation degrades as the RS codeword length decreases. Therefore, two ISD algorithm, namely the ISD-I and ISD-II, respectively, are proposed to decode RS-TBCC codes of various length. Our simulation results show that both the ISD-I and ISD-II of RS-TBCC codes yield a significant performance than the ISD of RS-CC codes.

## II. RS-TBCC CODES

Let  $\mathbb{F}_q = \{\rho_0, \rho_1, \dots, \rho_{q-1}\}$  denote the finite field of size  $q$ , which is assumed to be an extension field of  $\mathbb{F}_2$ , i.e.,  $q = 2^\omega$

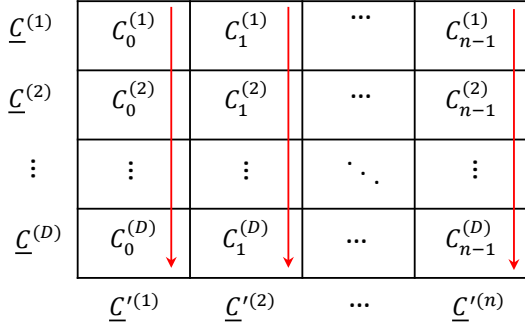


Fig. 2. Block interleaver.

where  $\omega$  is a positive integer. An RS code of length  $n = 2^\omega - 1$  and dimension  $k$  is denoted as an  $(n, k)$  RS code.

Fig. 1 shows an RS-TBCC code formed by encoding a sequence of  $D$  interleaved RS codewords with an inner TBC code. Given an  $(n, k)$  RS code of rate  $k/n$ ,  $D \times k$  information symbols form the message  $\underline{U} = [\underline{U}^{(1)} \underline{U}^{(2)} \dots \underline{U}^{(D)}]$ , where  $\underline{U}^{(\iota)} = [U_0^{(\iota)} U_1^{(\iota)} \dots U_{k-1}^{(\iota)}]$  is the  $\iota$ -th information sequence, and  $1 \leq \iota \leq D$ . Let

$$\mathbf{G} = \begin{bmatrix} 1 & 1 & \dots & 1 \\ 1 & \alpha & \dots & \alpha^{n-1} \\ \vdots & \vdots & \ddots & \vdots \\ 1 & \alpha^{k-1} & \dots & \alpha^{(k-1)(n-1)} \end{bmatrix} \quad (1)$$

denote the generator matrix of the RS code, where  $\alpha$  is a primitive element of  $\mathbb{F}_q$ . As shown in Fig. 1,  $\underline{U}$  will be encoded into  $\underline{C} = [\underline{C}^{(1)} \underline{C}^{(2)} \dots \underline{C}^{(D)}]$ , where each RS codeword  $\underline{C}^{(\iota)} = \underline{U}^{(\iota)} \times \mathbf{G} = [C_0^{(\iota)} C_1^{(\iota)} \dots C_{n-1}^{(\iota)}]$ .

Due to the nature of convolutional codes, burst errors will often be produced by the inner decoding. To better cope with burst errors, block interleaver is needed to interleave  $\underline{C}$  as Fig. 2 shows into

$$\underline{C}' = [C_0^{(1)} \dots C_0^{(D)} C_1^{(1)} \dots C_1^{(D)} \dots C_{n-1}^{(D)}], \quad (2)$$

which will then be converted into the binary string  $\underline{b}$  of length  $N = Dn\omega$ . Finally, binary string  $\underline{b}$  is the input of the TBC encoder, which yields a binary RS-TBCC codeword  $\underline{c}$ .

For simplicity, this paper considers the TBC code with 1 input, 2 outputs, and  $m$  shift registers, denoted as the  $(2, 1, m)$  TBC code. Hence, the length of codeword  $\underline{c}$  is  $2N$ . It should be noted that the overall RS-TBCC code rate is  $\frac{1}{2} \cdot \frac{k}{n}$ , while with the same component codes the overall RS-CC code rate is  $\frac{1}{2} \cdot \frac{\omega Dk}{N+m}$ . It can be seen that the latter suffers a rate loss in comparison with the RS-TBCC code.

### III. ITERATIVE SOFT DECODING I

Fig. 3 shows the proposed ISD-I for RS-TBCC codes, where  $\underline{P}$  and  $\underline{P}^*$  denote the input/output probability sequences of

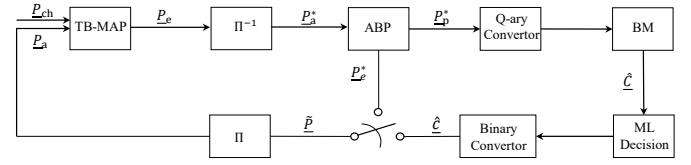


Fig. 3. Block diagram of the ISD-I.

the inner decoder and the outer decoders, respectively. For the probability sequence  $\underline{P} = [P_0 P_1 \dots P_{N-1}]$  (so as for  $\underline{P}^*$ ), its  $j$ -th element,  $P_j$ , denotes the probability mass function over  $\theta \in \{0, 1\}$  and  $P_j(\theta) = \Pr\{c_j = \theta\}$  denotes the probability of the outcome  $\theta$ , where  $j \in \{0, 1, \dots, N-1\}$ . Let  $\hat{\underline{C}}$  denote the BM decoding estimation (a non-binary vector) and  $\hat{c}$  denote its binary representation. With the channel observations  $\underline{P}_{\text{ch}} = [P_{\text{ch},0} P_{\text{ch},1} \dots P_{\text{ch},2N-1}]$  and the *a priori* probabilities  $\underline{P}_a = [P_{a,0} P_{a,1} \dots P_{a,N-1}]$  of the RS-TBCC coded bits, the TB-MAP decoder determines the extrinsic probabilities  $\underline{P}_e = [P_{e,0} P_{e,1} \dots P_{e,N-1}]$  of the RS coded bits by

$$P_{e,j}(\theta) = \varpi \frac{P_{p,j}(\theta)}{P_{a,j}(\theta)}, \quad (3)$$

where  $\varpi$  is a normalization factor that ensures  $P_{e,j}(0) + P_{e,j}(1) = 1$  and  $\underline{P}_p = [P_{p,0}, P_{p,1}, \dots, P_{p,N-1}]$  is the *a posteriori* probabilities determined by the TB-MAP decoder. Then,  $\underline{P}_e$  will be deinterleaved<sup>1</sup> and mapped to the *a priori* probabilities  $\underline{P}_a^* = [P_a^{*(1)} P_a^{*(2)} \dots P_a^{*(D)}]$  for the outer ABP decoder, where  $\underline{P}_a^{*(\iota)} = [P_{a,0}^{*(\iota)} P_{a,1}^{*(\iota)} \dots P_{a,N-1}^{*(\iota)}]$  are the *a priori* probabilities of all coded bits of the  $\iota$ -th RS codeword. For all  $1 \leq \iota \leq D$ , the ABP decoder utilizes  $\underline{P}_a^{*(\iota)}$  to determine the extrinsic probabilities  $\underline{P}_e^{*(\iota)}$  and the *a posteriori* probabilities  $\underline{P}_p^{*(\iota)}$  of the RS coded bits. The hard-decisions of  $\underline{P}_p^{*(\iota)}$  are then converted to the symbol wise received word and decoded by the BM algorithm [12]. If the BM decoding succeeds, it estimates an RS codeword  $\hat{\underline{C}}^{(\iota)}$ . Its binary representation  $\hat{c}^{(\iota)}$  can be further obtained, in which  $\hat{c}_j^{(\iota)}$  denotes its  $j$ -th bit, where  $0 \leq j \leq \omega n - 1$ . Let  $\tilde{\underline{P}}^{(\iota)} = [\tilde{P}_0^{(\iota)} \tilde{P}_1^{(\iota)} \dots \tilde{P}_{\omega n - 1}^{(\iota)}]$ . It can be updated based on the following rule: if  $\hat{\underline{C}}^{(\iota)}$  satisfies the ML criterion [11],  $\tilde{P}_j^{(\iota)}(\hat{c}_j^{(\iota)}) = 1$  and  $\tilde{P}_j^{(\iota)}(1 - \hat{c}_j^{(\iota)}) = 0, \forall j$ ; Otherwise,  $\tilde{P}_j^{(\iota)} = P_{e,j}^{*(\iota)}$ . Finally, by interleaving  $\tilde{\underline{P}}$ , we can obtain the updated *a priori* probabilities  $\underline{P}_a$  for the TB-MAP decoder in the next iteration. The iterative decoder will be terminated if all outer codewords  $\hat{\underline{C}}^{(\iota)}$  satisfy the ML criterion or the maximum iteration number is reached.

We then describe the TB-MAP decoder, the ABP decoder and the ML criterion to substantiate ISD-I algorithm.

<sup>1</sup>During deinterleaving, every  $\omega$  consecutive extrinsic probabilities are grouped to represent the extrinsic information of an RS coded symbol.

### A. TB-MAP Decoding of the Inner TBC Code

The TB-MAP decoder performs the BCJR algorithm [13] with the following two modifications: 1) The BCJR algorithm is performed over the supertrellis [9] of the TBC code, in which the supertrellis has  $2^m$  equal-probable initial states; 2) Given a wrap depth  $w$ , which is the length of the extended supertrellis [8], the TB-MAP decoder determines the extrinsic probabilities using (3) from the wrap-around channel observations  $\underline{P}_{\text{ch}}^{\text{wrap}}$  and the wrap-around *a priori* probabilities  $\underline{P}_{\text{a}}^{\text{wrap}}$ , where

$$\underline{P}_{\text{ch}}^{\text{wrap}} = [P_{\text{ch},0} P_{\text{ch},1} \cdots P_{\text{ch},2N-1} P_{\text{ch},0} \cdots P_{\text{ch},2w-1}], \quad (4)$$

$$\underline{P}_{\text{a}}^{\text{wrap}} = [P_{\text{a},0} P_{\text{a},1} \cdots P_{\text{a},N-1} P_{\text{a},0} \cdots P_{\text{a},w-1}]. \quad (5)$$

It should be noted that  $\underline{P}_{\text{ch}}^{\text{wrap}}$  and  $\underline{P}_{\text{a}}^{\text{wrap}}$  are circularly extended from  $\underline{P}_{\text{ch}}$  and  $\underline{P}_{\text{a}}$ , respectively.

From  $\underline{P}_{\text{ch}}^{\text{wrap}}$  and  $\underline{P}_{\text{a}}^{\text{wrap}}$ , the TB-MAP decoder determines the wrap-around extrinsic probabilities

$$\underline{P}_{\text{e}}^{\text{wrap}} = [P_{\text{e},0} P_{\text{e},1} \cdots P_{\text{e},N-1} P_{\text{e},N} \cdots P_{\text{e},N+w-1}] \quad (6)$$

using (3) and outputs the last  $N$  probabilities of  $\underline{P}_{\text{e}}^{\text{wrap}}$  as

$$\underline{P}_{\text{e}} = [P_{\text{e},N} \cdots P_{\text{e},N+w-1} P_{\text{e},w} P_{\text{e},w+1} \cdots P_{\text{e},N-1}]. \quad (7)$$

To approach the ML performance of TBC codes, the wrap depth  $w$  needs to be sufficiently large [8], which cause an additional decoding complexity. For example, the (2, 1, 6) TBC code of message length 48 needs a wrap depth of 40 to reach the optimal performance [9]. A wrap depth of  $6(m+1)$  for the TB-MAP decoder can yield a sufficiently superior performance, which will be adopted in this paper.

### B. ABP Decoding of the Outer RS Codes

Based on the *a priori* probabilities  $\underline{P}_{\text{a}}^{*(\ell)}$ , the log likelihood ratio (LLR) of the  $j$ -th bit of the  $\ell$ -th RS codeword is

$$L_{\text{a},j}^{(\ell)} = \log \frac{P_{\text{a},j}^{*(\ell)}(0)}{P_{\text{a},j}^{*(\ell)}(1)}, \quad (8)$$

where  $j \in \{0, 1, \dots, \omega n - 1\}$ . At the beginning, the ABP algorithm sorts the *a priori* LLR values based on their magnitudes in an ascending order, yielding a refreshed bit indices  $j_0, j_1, \dots, j_{\omega n - 1}$ . It indicates that  $|L_{\text{a},j_0}^{(\ell)}| \leq |L_{\text{a},j_1}^{(\ell)}| \leq \dots \leq |L_{\text{a},j_{\omega n - 1}}^{(\ell)}|$ . Let  $\Theta^{(\ell)} = \{j_0, j_1, \dots, j_{\omega(n-k)-1}\}$  denote the index set of the  $\omega(n-k)$  unreliable bits and  $\mathbf{H}_{\text{b}}$  denote an  $\omega(n-k) \times \omega n$  binary parity-check matrix of the RS code. Due to its density, Gaussian elimination will be needed to reduce the columns indexed by  $\Theta^{(\ell)}$  into weight-1, forming an adapted parity-check matrix  $\mathbf{H}'_{\text{b}}$  [10]. By doing so, density of  $\mathbf{H}_{\text{b}}$  can be reduced, so as the number of short cycles. Consequently, propagation of the unreliable information can be alleviated, resulting in a better BP decoding performance for RS codes. The BP decoding [10] based on  $\mathbf{H}'_{\text{b}}$  can be described as follows.

Let  $h_{v,j}$  denote the entry of  $\mathbf{H}'_{\text{b}}$ ,

$$\mathbf{V}(j) = \{v | h_{v,j} = 1, \forall v = 0, 1, \dots, \omega(n-k) - 1\} \quad (9)$$

and

$$\mathbf{J}(v) = \{j | h_{v,j} = 1, \forall j = 0, 1, \dots, \omega n - 1\}. \quad (10)$$

The extrinsic LLR for each RS coded bit is determined [10] by

$$L_{\text{e},j}^{(\ell)} = \sum_{v \in \mathbf{V}(j)} 2 \tanh^{-1} \left( \prod_{j' \in \mathbf{J}(v) \setminus \{j\}} \tanh \left( \frac{L_{\text{a},j'}^{(\ell)}}{2} \right) \right). \quad (11)$$

The *a posteriori* LLR of the each RS coded bit is further determined by

$$L_{\text{p},j}^{(\ell)} = L_{\text{a},j}^{(\ell)} + \eta L_{\text{e},j}^{(\ell)}, \quad (12)$$

where  $\eta \in (0, 1]$  is the damping factor that downgrades the extrinsic influence. Finally, the outputs of the ABP decoder,  $\underline{P}_{\text{p}}^{*(\ell)}$  and  $\underline{P}_{\text{e}}^{*(\ell)}$ , can be determined by

$$P_{\text{p},j}^{*(\ell)}(\theta) = \frac{1}{1 + e^{(2\theta-1)L_{\text{p},j}^{(\ell)}}}, \quad (13)$$

and

$$P_{\text{e},j}^{*(\ell)}(\theta) = \frac{1}{1 + e^{(2\theta-1)L_{\text{e},j}^{(\ell)}}}, \quad (14)$$

respectively. It should be noted that the ABP decoder itself is also iterative. By mapping

$$\underline{L}_{\text{p}}^{(\ell)} \mapsto \underline{L}_{\text{a}}^{(\ell)}, \quad (15)$$

another round of reliability sorting, Gaussian elimination and BP iterations will be performed.

### C. ML Criterion of the Outer Decoding Output

With the knowledge of the *a posteriori* probabilities  $\underline{P}_{\text{p}}^*$  from ABP decoding, the reliability matrix  $\mathbf{\Pi} \in \mathbb{R}^{q \times n}$  w.r.t an RS codeword  $\hat{\mathbf{C}}$  can be formed. Its entry  $\pi_{\iota,j}$  can be considered as an *a priori* probability of an RS codeword symbol  $\hat{C}_j$  being the field symbol  $\rho_{\iota}$  where  $\iota \in \{0, 1, \dots, q-1\}$  and  $j \in \{0, 1, \dots, n-1\}$ . Let  $\Xi_{\iota}$  denote the binary representation of field symbol  $\rho_{\iota}$  and

$$\Xi_{\iota} = [\theta_1 \theta_2 \dots \theta_{\omega} | \rho_{\iota}] = \sum_{\varsigma=1}^{\omega} \theta_{\varsigma} \alpha^{\omega-\varsigma}, \theta_{\varsigma} \in \{0, 1\}. \quad (16)$$

This symbol wise *a posteriori* probability  $\pi_{\iota,j}$  can be determined by

$$\pi_{\iota,j} = \Pr\{C_j = \rho_{\iota}\} = \prod_{\theta_{\varsigma} \in \Xi_{\iota}} P_{\text{p},(j-1)\omega+\varsigma}^*(\theta_{\varsigma}). \quad (17)$$

The ML decoding is to find a codeword  $\hat{\mathbf{C}}$  that maximizes metric  $\sum_{0 \leq j \leq n-1} \log(\pi_{\zeta_j,j})$ , where  $\zeta_j = \text{index}\{\zeta | \rho_{\zeta} = \hat{C}_j\}$ . Let  $\pi_j^{1\text{st}}$  and  $\pi_j^{2\text{nd}}$  denote the largest and the second largest values in the  $j$ -th column of  $\mathbf{\Pi}$ , respectively, we have

$$\sum_{0 \leq j \leq n-1} \log(\pi_{\zeta_j,j}) = \sum_{0 \leq j \leq n-1} \log(\pi_j^{1\text{st}}) - \sum_{j: \hat{C}_j \neq \hat{R}_j} (\log(\pi_j^{1\text{st}}) - \log(\pi_{\zeta_j,j})), \quad (18)$$

TABLE I  
STATISTICS OF THE ML VALIDATION.

RS codes	Percentage of satisfying (21)	Percentage of errors
(7, 5)	98.907%	1.04%
(15, 11)	99.450%	0.196%

where  $\hat{\underline{R}} = [\hat{R}_0, \hat{R}_1, \dots, \hat{R}_{n-1}]$  is the hard-decision received word estimated based on  $\Pi$ .

Therefore, the ML decoding is to find a codeword  $\hat{\underline{C}}$  that minimizes the metric

$$l(\hat{\underline{R}}, \hat{\underline{C}}) = \sum_{j: \hat{C}_j \neq \hat{R}_j} (\log(\pi_j^{1st}) - \log(\pi_{\hat{C}_j, j})). \quad (19)$$

Reordering all the elements in  $\{\log(\pi_j^{1st}) - \log(\pi_j^{2nd}) : \hat{C}_j = \hat{R}_j\}$  as  $\log(\pi_{j_1}^{1st}) - \log(\pi_{j_1}^{2nd}) \leq \log(\pi_{j_2}^{1st}) - \log(\pi_{j_2}^{2nd}) \leq \dots$ , we can define

$$\tilde{l}(\hat{\underline{R}}, \hat{\underline{C}}) = \sum_{\varsigma=1}^{d_{\min}-d} (\log(\pi_{j_\varsigma}^{1st}) - \log(\pi_{j_\varsigma}^{2nd})), \quad (20)$$

where  $d_{\min} = n - k + 1$  is the minimum Hamming distance of the code and  $d$  is the Hamming distance between  $\hat{\underline{R}}$  and  $\hat{\underline{C}}$ . The following lemma [11] can be used to identify the most likely transmitted codeword.

**lemma 1:**

If a codeword  $\hat{\underline{C}}$  satisfies

$$l(\hat{\underline{R}}, \hat{\underline{C}}) \leq \tilde{l}(\hat{\underline{R}}, \hat{\underline{C}}), \quad (21)$$

then there is no codeword which is more likely than  $\hat{\underline{C}}$ .

#### IV. ITERATIVE SOFT DECODING II

This research has noticed that when the RS codeword length decreases, effectiveness of the above ML criterion also degrades. That says a estimated codeword  $\hat{\underline{C}}$  that satisfies the inequality of **lemma 1** will exhibit a higher probability of not matching the transmitted codeword. This will result in the fed back deterministic probabilities being erroneous, affecting the following iterations. Table I shows some statistics in validating the RS code using the ML criterion of **lemma 1** over the additive white Gaussian noise (AWGN) channel at the signal-to-noise ratio (SNR) of 4 dB. It can be seen that for both the (15, 11) and (7, 5) RS codes, there exhibits a similar percentage of an ABP-BM output that satisfies the ML criterion. However, for the shorter code, its percentage of a validated codeword not matching the transmitted one is noticeably higher. This will make the above ISD-I algorithm more likely to feedback the erroneous deterministic probabilities. This will pose a negative impact for the iterative decoding system.

Therefore, the ISD-II algorithm that is illustrated as in Fig. 4 is further proposed for RS-TBCC codes in which the outer codes are short. In ISD-II, the inner TB-MAP decoding and the outer ABP decoding iterate extrinsic probabilities of the RS coded bits without accommodating the deterministic probabilities in the iterations. Unlike the ISD-I that validates individual

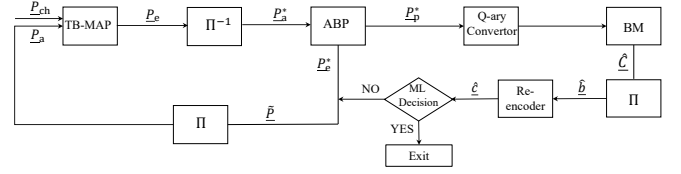


Fig. 4. Block diagram of the ISD-II.

RS codeword, it validates an entire RS-TBCC codeword once all outer RS codes are decoded (the BM algorithm produces an estimation). If the ML criterion that stated below is satisfied, the decoding will be terminated. Otherwise, the TB-MAP and ABP iteration continues. The decoding will also be terminated if the maximum iteration number is reached.

We denote the reliability of the  $j$ -th RS-TBCC coded bit as  $|\phi_j|$  and the hard-decision of  $\phi_j$  as  $r_j$ , where  $\phi_j = \log \frac{P_{ch,j}(0)}{P_{ch,j}(1)}$ ,  $\forall j = 0, 1, \dots, 2N - 1$ . The ML decoding of RS-TBCC codes is to find a  $\hat{\underline{c}}$  that maximizes

$$\sum_{j: \hat{c}_j = \hat{r}_j} |\phi_j| - \sum_{j: \hat{c}_j \neq \hat{r}_j} |\phi_j| = \sum_{0 \leq j \leq 2N-1} |\phi_j| - 2 \sum_{j: \hat{c}_j \neq \hat{r}_j} |\phi_j|, \quad (22)$$

which is equivalent to minimize

$$l(\hat{\underline{r}}, \hat{\underline{c}}) \triangleq \sum_{j: \hat{c}_j \neq \hat{r}_j} |\phi_j|. \quad (23)$$

We then reorder all the elements in  $\{|\phi_j| : \hat{c}_j = \hat{r}_j\}$  as  $|\phi_{j_1}| \leq |\phi_{j_2}| \leq \dots \leq |\phi_{j_{\tilde{d}-1}}|$  and define

$$\tilde{l}(\hat{\underline{r}}, \hat{\underline{c}}) = \sum_{\varsigma=1}^{\tilde{d}_{\min}-\tilde{d}} |\phi_{j_\varsigma}|, \quad (24)$$

where  $\tilde{d}_{\min}$  is the minimum Hamming distance of the RS-TBCC code and  $\tilde{d}$  is the Hamming distance between  $\hat{\underline{r}}$  and  $\hat{\underline{c}}$ . We can use the following lemma [11] to identify the most likely transmitted codeword.

**lemma 2:**

If a codeword  $\hat{\underline{c}}$  satisfies

$$l(\hat{\underline{r}}, \hat{\underline{c}}) \leq \tilde{l}(\hat{\underline{r}}, \hat{\underline{c}}), \quad (25)$$

then there is no codeword which is more likely than  $\hat{\underline{c}}$ .

It should be noted that the minimum Hamming distance of the RS-TBCC code is approximated as the product of the minimum Hamming distance of the RS codes and the TBC code [14].

#### V. SIMULATION RESULTS

This section shows the performances of the RS-CC and RS-TBCC codes over the AWGN channel using BPSK. The RS-TBCC code is compared with the RS-CC code. We consider the (15, 11) RS code and the (7, 5) RS code concatenated with the TBC code of  $m = 10$  with the generator polynomials of  $[6472, 7542]_8$  (in octal form) [15]. For the convolutional code of  $m = 10$ , its generator polynomials are  $[2473, 3217]_8$  [16]. In decoding the outer RS codes, there are 2 ABP iterations

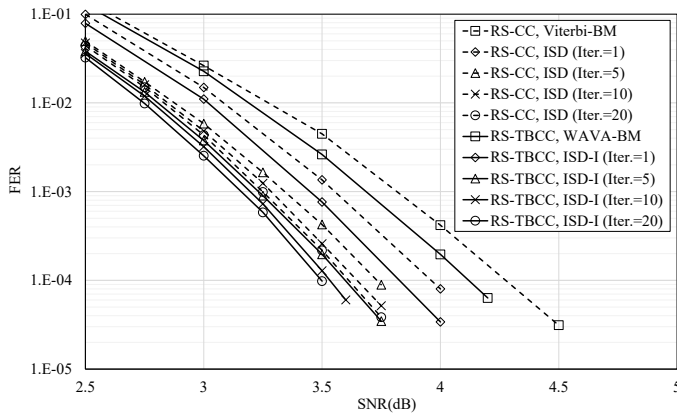


Fig. 5. ISD-I performance of RS-TBCC code.

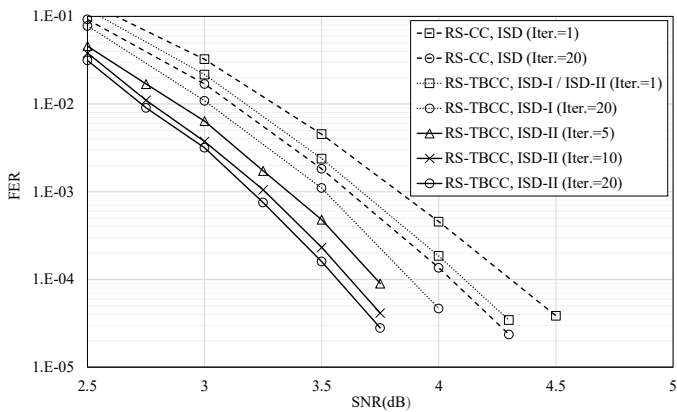


Fig. 6. ISD-I and ISD-II performance of RS-TBCC code.

and 2 BP iterations performed on each reduced matrix  $\mathbf{H}'_b$  with a damping factor 0.3.

Fig. 5 shows the frame error rate (FER) of all simulated codes with  $m = 10$  and  $D = 4$  using the (15, 11) RS code as the outer codes. The RS-CC code would be decoded by the Viterbi-BM decoder and the iterative soft decoder (ISD), while the RS-TBCC code would be decoded by the WAVA-BM decoder [8] and the proposed ISD-I. Fig. 5 shows the iterative decoding algorithms can outperform their non-iterative counterparts. E.g., for RS-TBCC codes, the ISD-I outperforms the WAVA-BM with a performance gain improved by increasing the maximal number of global iterations for the concatenated code. Moreover, the RS-TBCC code can also outperform the RS-CC code, due to its advantage in avoiding rate loss.

Fig. 6 shows the FER of the RS-TBCC code with  $m = 10$  and  $D = 8$ , using the (7, 5) RS code as the outer codes. The RS-TBCC codes would be decoded by the ISD-I and the ISD-II, respectively. Fig. 6 shows that the RS-TBCC code can still outperform the RS-CC code. With a less iteration number, the ISD-II algorithm substantially outperforms the ISD-I algorithm. This demonstrates the fact that the ML criterion of *lemma 1* becomes less effective for assess the

BM decoding output of the (7, 5) RS code. The ISD-II algorithm that assesses the ML property of the entire RS-TBCC codeword will be more effective in decoding the RS-TBCC code.

## VI. CONCLUSION

This paper has proposed the ISD algorithms for RS-TBCC codes in maximizing the codes' performance. The iterative decoders are constituted by the TB-MAP algorithm and the ABP-BM algorithm for the inner code and the outer codes, respectively. The primary ISD-I algorithm realizes iterative decoding gains for the RS-TBCC code and enables its advantage over the RS-CC code. The secondary ISD-II algorithm has been further designed for cases with very short outer codes.

## ACKNOWLEDGMENT

This work is sponsored by National Natural Science Foundation of China (NSFC) with project ID 61671486.

## REFERENCES

- [1] M. Agiwal, A. Roy, and N. Saxena, "Next generation 5G wireless networks: A comprehensive survey," *IEEE Comm. Surveys Tutorials*, vol. 18, no. 3, pp. 1617–1655, 2016.
- [2] P. Popovski, K. F. Trillingsgaard, O. Simeone, and G. Durisi, "5G wireless network slicing for eMBB, URLLC, and mMTC: A communication-theoretic view," *IEEE Access*, vol. 6, pp. 55 765–55 779, 2018.
- [3] M. C. Coskun, G. Durisi, T. Jerkovits, G. Liva, W. Ryan, B. Stein, and F. Steiner, "Efficient error-correcting codes in the short blocklength regime," *Physical Comm.*, vol. 34, no. JUN., pp. 66–79, 2019.
- [4] R. L. Miller, L. J. Deutsch, and S. A. Butman, "On the error statistics of Viterbi decoding and the performance of concatenated codes," *JPL Pub.*, Sep. 1981.
- [5] H. Ma and J. Wolf, "On tail biting convolutional codes," *IEEE Trans. Comm.*, vol. 34, no. 2, pp. 104–111, 1986.
- [6] G. Schmidt, C. Senger, V. R. Sidorenko, and M. Bossert, "Concatenated code designs with outer interleaved Reed-Solomon codes and inner tailbiting convolutional codes," in *7th International ITG Conf. SCC*, 2008.
- [7] L. Chen, "Iterative soft decoding of Reed-Solomon convolutional concatenated codes," *IEEE Trans. Comm.*, vol. 61, no. 10, pp. 4076–4085, Oct. 2013.
- [8] R. Y. Shao, S. Lin, and M. P. Fossorier, "Two decoding algorithms for tailbiting codes," *IEEE Trans. Comm.*, vol. 51, no. 10, pp. 1658–1665, 2003.
- [9] J. B. Anderson and S. M. Hladik, "Tailbiting map decoders," *IEEE J. Selected Areas Comm.*, vol. 16, no. 2, pp. 297–302, Feb. 1998.
- [10] J. Jiang and K. R. Narayanan, "Iterative soft-input soft-output decoding of Reed-Solomon codes by adapting the parity-check matrix," *IEEE Trans. Inform. Theory*, vol. 52, no. 8, pp. 3746–3756, Aug. 2006.
- [11] T. Kaneko, T. Nishijima, H. Inazumi, and S. Hirasawa, "An efficient maximum-likelihood-decoding algorithm for linear block codes with algebraic decoder," *IEEE Trans. Inform. Theory*, vol. 40, no. 2, pp. 320–327, Mar. 1994.
- [12] J. Massey, "Shift-register synthesis and BCH decoding," *IEEE Trans. Inform. Theory*, vol. 15, no. 1, pp. 122–127, Jan. 1969.
- [13] L. Bahl, J. Cocke, F. Jelinek, and J. Raviv, "Optimal decoding of linear codes for minimizing symbol error rate," *IEEE Trans. Inform. Theory*, vol. 20, no. 2, pp. 284–287, Mar. 1974.
- [14] J. Justesen, C. Thommesen, and V. V. Zyablov, "Concatenated codes with convolutional inner codes," *IEEE Trans. Inform. Theory*, vol. 34, no. 5, pp. 1217–1225, 1988.
- [15] M. Agiwal, A. Roy, and N. Saxena, "Next generation 5G wireless networks: A comprehensive survey," *IEEE Comm. Surveys Tutorials*, vol. 18, no. 3, pp. 1617–1655, 2016.
- [16] I. F. Blake, "Error control coding by shu lin and daniel j. costello," *IEEE Trans. Inform. Theory*, 2005.